行政院國家科學委員會專題研究計畫　期中進度報告

金屬/具奈米結構半導體界面載子傳輸物理機制之研究

(1/3)

計畫類別：個別型計畫
計畫編號：NSC94-2112-M-018-007-
執行期間：94年08月01日至95年07月31日
執行單位：國立彰化師範大學光電科技研究所

計畫主持人：林祐仲

計畫參與人員：朱宥霖,林文祥,蔡佳龍,游長峯

報告類型：精簡報告

處理方式：本計畫可公開查詢

中　華　民　國 95年5月18日

研究計畫中文摘要：

關鍵字：歐姆接觸，蕭特基接觸，奈米結構

當材料的特徵尺度降低到奈米尺度時，會因小尺度效應、量子效應、界面和表面效應等影響，出現和巨觀世界裡材料之常規性質不同之特性。本計畫重點便是研究奈米材料和同質大型塊材的能階特性，利用乾蝕刻技術製作具奈米結構之半導體亦或是製作多孔氧化鋁模板再填充半導體材料製備奈米半導體材料，於完成後即進行各項光電特性觀測。本計畫在三年的時間內將逐步進行各項實驗：於第一年進行製作奈米半導體材料，並與同質大型塊材進行特性比較，深入探討奈米結構體之表面特性；第二年和第三年分別研究金屬/奈米材料之歐姆接觸與蕭特基接觸之物理機制及其界面載子傳輸行為，並建立新型之奈米尺度金屬/半導體界面理論。

研究計畫英文摘要：

Keywords： ohmic contact，Schottky contact，nanostructure

Nanostructured semiconductors are promising candidates for future electronic and photonic devices. As material size has diminished, the quality of these interfaces and surfaces has become an increasingly important concern. Additionally, due to quantum confinement effects, fabrication and studies of nanostructures have attracted considerable interest for potential application to electronic and optoelectronic devices. In this plan, we are devoted to provide the physical models for the ohmic and Schottky contacts, and the carrier transport at the metal/nanostructured semiconductor interface. The nanostructured semiconductors formed via dry etching or grown with alumina nanopores templates will be used in our study.

第一年計畫成果自評：

本次計畫研究初步成果與原計畫相符程度達 70%，並達成初期目標，而且研究成果九篇論文均已發表於國際知名期刊，獲得國際學者肯定，極具學術與實際應用之價值。

研究報告內容：

此次三年專題計畫之第一年研究初步成果已撰寫成九篇論文並已發表在國際期刊，同時也完成六篇研討會論文，依序列於下：

國際期刊論文：

1. **Y. J. Lin,** 2006, Jan. “Nonalloyed ohmic formation for p-type AlGaN with p-type GaN capping layers using ohmic recessed technique”, Jpn. J. Appl. Phys. Vol. 45,

L86. (與本計劃研究內容相似度 80%)

2. **Y. J. Lin**, C. F. You, and C. S. Lee, 2006, March “Enhancement of Schottky barrier height on p-type GaN by $(NH_4)_2S_x$ treatment”, J. Appl. Phys. Vol.99, 053706. (與本計劃研究內容相似度 60%)
3. **Y. J. Lin,** W. X. Lin, C. T. Lee, and H. C. Chang, 2006, April “Electronic transport and Schottky barrier heights of Ni/Au contacts on n-type GaN surface with and without a thin native oxide layer”, Jpn. J. Appl. Phys. Vol.45, 2505. (與本計劃研究內容相似度 60%)
4. **Y. J. Lin**, W. X. Lin, C. T. Lee, and F. T. Chien, 2006, Feb. “Changes in optical and electrical properties and surface recombination velocity of n-type GaN due to $(NH_4)_2S_x$ treatment”, Solid State Communications. Vol.137, 257. (與本計劃研究內容相似度 50%)
5. **Y. J. Lin,** Y. L. Chu, D. S. Liu, C. S. Lee, and F. T. Chien, 2006, Jan. “Optical properties of heavily Mg-doped p-GaN films prepared by reactive ion etching”, Jpn. J. Appl. Phys. Part 1, Vol. 45, 64. (與本計劃研究內容相似度 50%)
6. **Y. J. Lin,** Y. L. Chu, W. X. Lin, F. T. Chien, and C. S. Lee, 2006, April “Induced changes in surface band bending of n-type and p-type AlGaN by oxidation and wet chemical treatments”, J. Appl. Phys. (與本計劃研究內容相似度 50%)
7. **Y. J. Lin**, C. L. Tsai, Y. M. Lu, and C. J. Liu, 2006, May “Optical and electrical properties of undoped ZnO films”, J. Appl. Phys. (與本計劃研究內容相似度 50%)
8. **Y. J. Lin,** W. Y. Chou, and S. T. Lin, 2006, Feb. **“**Enhanced efficiency in polymer light-emitting diodes due to the improvement of charge-injection balance**”,** Appl. Phys. Lett. 88, 071108. (與本計劃研究內容相似度 40%)
9. **Y. J. Lin,** W. Y. Chou, S. T. Lin, and Y. M. Chen, 2005, Sep. “Influence of KrF excimer laser irradiation on luminescent performance of polymer light-emitting diodes”, Jpn. J. Appl. Phys. Part 2, Vol. 44, L1218. (與本計劃研究內容相似度 40%)

研討會論文：

1. **Yow-Jon Lin**, 2006, Jan. 16-18 “Formation mechanisms of nonalloyed ohmic contacts to p-type AlGaN with the capping layer”, 2006 中華民國物理學會年會暨研究成果發表會, 台北, 台灣.
2. **林祐仲**, 2005, Nov. 24-25 “二維電洞氣在 P 型氮化鎵非熱合金化歐姆接觸形成中所扮演的角色”, 2005 大葉大學奈米技術與材料研討會, 彰化, 台灣.
3. Yow-Lin Chu and **Yow-Jon Lin**, 2005, Nov. 24-25 “Effects of reactive ion etching on optical and electrical properties of heavily Mg-doped p-type GaN”, 2005 年電子元件暨材料研討會,高雄,台灣.

4. 朱宥霖,**林祐仲**和黃鶯聲, 2005, Dec. 9-10 “硫化處理對鎂重摻雜的 P 型氮化鎵光電特性影響之研究”, 2005 台灣光電科技研討會,台南,台灣.
5. 林文祥,**林祐仲**和李清庭, 2005, Dec. 9-10 “經硫化銨處理之 n 型氮化鎵改變表面復合速率與其光電特性之研究” , 2005 台灣光電科技研討會,台南,台灣.
6. 蔡佳龍,**林祐仲**和盧陽明, 2005, Dec. 9-10 “未摻雜 ZnO 薄膜光電特性之研究” , 2005 台灣光電科技研討會,台南,台灣.

其中，列在發表於國際期刊之第一篇論文[Jpn. J. Appl. Phys. 45, L86 (2006)]以及於 2005 大葉大學奈米技術與材料研討會所發表之論文與本計劃研究內容相似度達 80%。發表於 Jpn. J. Appl. Phys. 45, L86 (2006)之論文報導 III 族氮化物異質結構間因壓電極化和自發極化效應，於異質界面形成約數奈米厚度之高電洞面密度，本研究利用挖掘通道技術與此界面累積高電洞面密度特性，成功地製作金屬/p 型 AlGaN 非熱合金化歐姆接觸，解決紫外光發光二極體或雷射二極體電極製作，文中亦詳細解釋如何利用異質結構所引發奈米厚度之二維電洞氣形成金屬/p 型 AlGaN 非熱合金化歐姆接觸之物理機制。

另外，發表於J. Appl. Phys. 99, 053706 (2006)之論文[列在發表於國際期刊之第二篇論文]報導p型GaN經$(NH_4)_2S_x$化學溶液處理後有效降低表面點缺陷，當金屬沉積後可形成較高之位障(barrier)，經分析驗證發現界面載子傳輸行為受熱游子場放射(thermionic field emission)機制所主導，此原因是p型GaN經$(NH_4)_2S_x$化學溶液處理後仍殘於大量受體型缺陷導致位障厚度較窄，增加載子穿遂機率。

再者，發表於Jpn. J. Appl. Phys. 45, 2505 (2006)之論文[列在發表於國際期刊之第二篇論文]報導n型GaN半導體經$(NH_4)_2S_x$化學溶液處理後有效去除表面原生氧化層(例如: GaO_x)並減少n型GaN表面態密度(surface state density)，當金屬沉積後可形成較高之位障，經電流-電壓法和電容-電壓法分析驗證發現界面載子傳輸行為屬熱游子放射(thermionic emission)。如果金屬直接沉積於具原生氧化層之n型GaN，其實驗結果指出界面載子傳輸行為受熱游子場放射機制所主導，此原因是原生氧化層/n型GaN界面存在大量界面態(interface states)，此界面態提供載子於界面傳輸時之穿遂路徑致使穿遂機率增加。

上述三篇發表在國際期刊之論文的詳細內容依序如下所示：

Japanese Journal of Applied Physics
Vol. 45, No. 3, 2006, pp. L86–L88
©2006 The Japan Society of Applied Physics

Nonalloyed Ohmic Formation for p-Type AlGaN with p-Type GaN Capping Layers Using Ohmic Recessed Technique

Yow-Jon LIN*

Institute of Photonics, National Changhua University of Education, Changhua 500, Taiwan, Republic of China

(Received August 25, 2005; accepted November 26, 2005; published online January 13, 2006)

In this study, we report that the p-type GaN (p-GaN) capping layer grown on top of p-type AlGaN (p-AlGaN) and the fabrication of recessed channels are used to demonstrate a new type of nonalloyed ohmic contact. Because the p-GaN layer grown on p-AlGaN led to the formation of spontaneous polarization fields in p-GaN and the lower band bending of p-AlGaN resulting in the formation of a two-dimensional hole gas (2DHG). As a result, we deduce that holes can be easily injected into the p-AlGaN layer through recessed channels and a 2DHG channel, which results in nonalloyed ohmic formation.
[DOI: 10.1143/JJAP.45.L86]

KEYWORDS: AlGaN, ohmic contact, GaN, specific contact resistance, two-dimensional hole gas

In recent years, there has been a great effort to develop III-nitride-based light emitters and lasers[1–6] that have the potential to cover the wavelength range from red through green to UV. Interest is growing to extend the range of light emission of these devices deeper into the UV by incorporating more Al-rich AlGaN composition. UV light-emitting diodes (LEDs) with emission wavelengths below 340 nm have many important applications, including biological and chemical agent detection, high-density data storage, and air–water purification and medical usage.[7] For achieving high-quality performance of these devices, low-resistance ohmic contacts are essential. However, it is difficult to obtain ohmic contacts on p-type AlGaN (p-AlGaN) due to the wide band gap and high work function of p-AlGaN and the absence of metals having a work function larger than that of p-AlGaN. Reported ohmic contacts on p-AlGaN have been achieved using a metallization scheme (annealing at a high temperature).[8–11] However, annealing at a high temperature has been suspected as the cause of degradation in device performance. To our knowledge, a nonalloyed ohmic contact on p-AlGaN has not been reported. On the basis of the theory of polarization-enhanced ohmic contacts using a capping layer,[12–14] we develop ohmic recessed technology for nonalloyed low-resistance ohmic contacts on p-AlGaN in this letter.

The epitaxial layers used in the study were grown on *c*-plane sapphire substrates. Trimethylgallium, trimethylaluminum, ammonia, and bis-cyclopentadienylmagnesium were used as Ga, Al, N, and Mg sources, respectively. An undoped AlN buffer layer was grown on a sapphire substrate, followed by the growth of a Mg-doped p-AlGaN layer (500 nm). Because of the known benefits of using an AlN epilayer as a template for nitride devices and its excellent UV transparency down to 200 nm, the insertion of an AlN epilayer as a template becomes a natural choice.[15] Then, a Mg-doped p-type GaN (p-GaN) capping layer (10 nm) was grown on top of p-AlGaN. Mg doping concentration in p-GaN and p-AlGaN was fixed at $2 \times 10^{19}\,\mathrm{cm}^{-3}$. The Al mole fraction in p-AlGaN was set at 0.2. To observe the carrier concentration and the mobility of the p-AlGaN layer, a sample grown without the p-GaN capping layer was prepared in this study. After activation annealing at 750°C

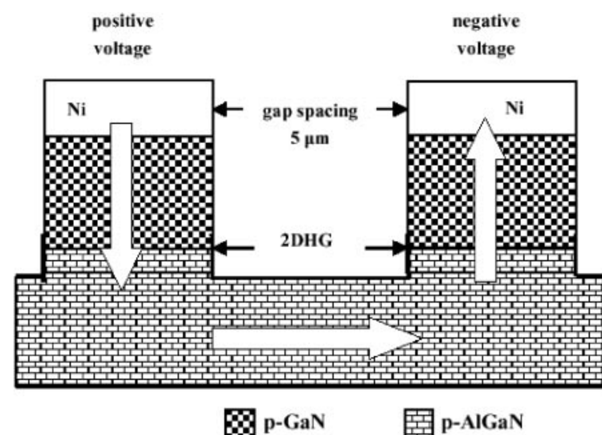

Fig. 1. Cross section of a sample structure without recessed channels for TLM measurements. White arrow: direction of hole current.

for 30 min in atmospheric N_2, a carrier concentration of $1.7 \times 10^{17}\,\mathrm{cm}^{-3}$ and a mobility of $3.2\,\mathrm{cm}^2/(\mathrm{V\,s})$ were obtained by room-temperature Hall measurement. A further description of the fabrication procedure of Ni nonalloyed ohmic contacts on p-AlGaN will be given later.

Figure 1 shows the sample structure without recessed channels (referred to as group A) for transmission line method (TLM)[16,17] measurements. Figure 2 shows the schematic band diagram for samples from group A.[12] Figure 3 shows the sample structure with recessed channels (referred to as group B) for TLM measurements. Figure 4 shows the vertical view for a sample structure with recessed channels for TLM measurements. The fabrication process of TLM patterns was reported in ref. 16. The dimensions of the p-pad electrode in the TLM pattern were $100 \times 100\,\mu\mathrm{m}^2$. Recessed channels, as shown in Fig. 3, were formed using the lift-off and reactive ion etching (RIE) technique, prior to the deposition of Ni using an electron beam evaporator. The p-GaN capping layers between the contacts in the TLM patterns were simultaneously removed during the etching process. The samples were etched by RIE technique in BCl_3 plasma with an rf power of 150 W. During the etching process, the BCl_3 flow rate was 5 sccm (standard cubic centimeter per minute) and the chamber pressure was 4 Pa. After etching, the samples were dipped into aqua regia for 10 min to remove the metallic mask. Then, the samples with

*Corresponding author. E-mail address: rzr2390@yahoo.com.tw

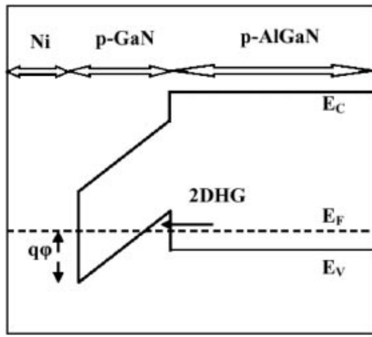

Fig. 2. Schematic band diagram for samples from group A. E_C: conduction band edge, E_V: valence band edge, E_F: Fermi energy, and $q\varphi$: barrier height at Ni/p-GaN interfaces.

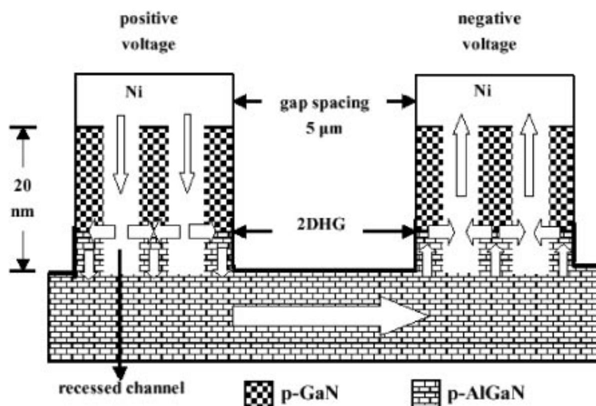

Fig. 3. Cross section of sample structure with recessed channels for TLM measurements. White arrow: direction of hole current.

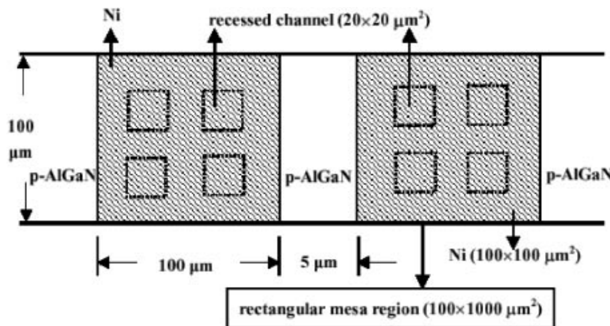

Fig. 4. Vertical view for sample structure with recessed channels for TLM measurements.

and without etching were annealed at 750°C for 30 min in atmospheric N_2 for dopant activation and removal of induced defects by RIE etching. For etched samples, we can see that the length and cross-sectional area of recessed channels are 20 nm and $20 \times 20\,\mu m^2$, respectively, as shown in Figs. 3 and 4. In Fig. 4, we can also see that four recessed channels per contact in the TLM pattern were formed.

Figure 5 shows the respective current–voltage (I–V) characteristics of samples from groups A and B, measured between p-pad electrodes with a gap spacing (d) of 5 μm. The least-squares linear regression and TLM data are shown in the inset of Fig. 5. The I–V characteristics of the TLM patterns were measured using a Keithley Model-4200-SCS/

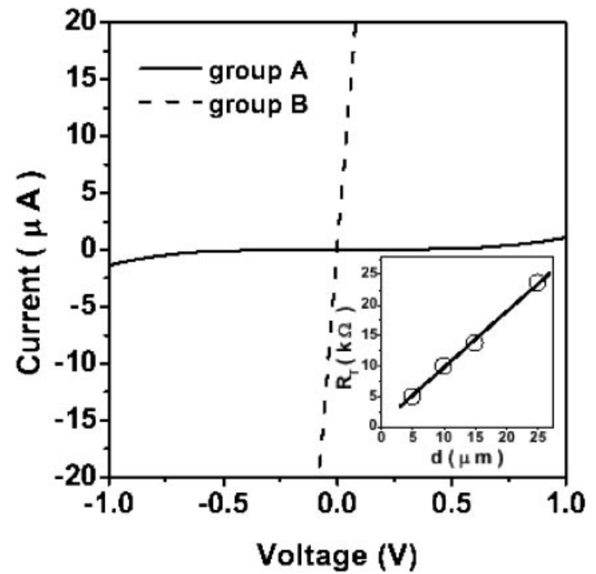

Fig. 5. I–V characteristics of samples from groups A and B. The inset panel shows the least-squares linear regression and TLM data.

F semiconductor characterization system. In Fig. 5, we find that the I–V characteristics of samples from group B are better than those of samples from group A and the samples from group B show a linear I–V behavior with a specific contact resistance (ρ_c), $1.1 \times 10^{-4}\,\Omega\,cm^2$. The associated ρ_c was obtained from the TLM model.[16,17] The total resistance (R_T) between any contacts is expressed as[17]

$$R_T = (\rho_s d/Z) + 2R_c \approx (\rho_s/Z)(d + 2L_T), \qquad (1)$$

where R_c is the contact resistance, ρ_s is the sheet resistance, Z is the contact width ($Z = 100\,\mu m$), and L_T is the transfer length. The intercept at $d = 0$ is $R_T = 2R_c$ giving the contact resistance and the slope of the plot is equal to ρ_s/Z giving the sheet resistance. According to the result shown in the inset of Fig. 5, we find $R_c = 316\,\Omega$, $L_T = 347$ nm, and $\rho_s = 91011\,\Omega/\square$. According to the result reported by Gessemann *et al.*,[12] the p-GaN capping layer grown on top of p-AlGaN led to the formation of spontaneous polarization fields in the p-GaN capping layer and the lower band bending of p-AlGaN resulting in the formation of a two-dimensional hole gas (2DHG), as shown in Fig. 2. As a result, the concentration of free holes at the p-GaN/p-AlGaN interface is markedly increased and the lower band bending of p-AlGaN at the p-GaN/p-AlGaN interface is formed,[12,13] thereby allowing for the enhancement of the hole injection in the p-AlGaN layer through the recessed channels in the p-GaN/p-AlGaN sample and the 2DHG channel at the p-GaN/p-AlGaN interface (shown in Figs. 3 and 2). This can explain why the sample from group B shows a linear I–V behavior. However, for samples from group A, we find that the high barrier at the Ni/p-GaN interface may impede the hole injection in the p-AlGaN layer resulting in nonlinear I–V behavior, as shown in Figs. 2 and 5.

On the other hand, we found that the barrier height at the Ni/p-GaN interface is equal to 1.9 eV reported in a previous study.[18] In addition, we demonstrated that RIE could be useful for the formation of higher barrier at the metals/etched p-GaN interface, as shown in ref. 19. Due to the high barrier existing at the Ni/p-GaN, Ni/etched p-GaN, Ni/p-

AlGaN or Ni/etched p-AlGaN interfaces, it is difficult for hole injection to occur from Ni to p-GaN or from Ni to p-AlGaN. Therefore, holes could be easily injected into the p-AlGaN layer through the recessed channels and the 2DHG channel at the p-GaN/p-AlGaN interface, as shown in Fig. 3. Furthermore, for samples with recessed channels (group B), the actual contact area for current flow across the interface may be smaller than the square contact area ($100 \times 100\,\mu m^2$) of the p-pad electrode in the TLM patterns. Therefore, the real interface impedance might be lower than the measured value.

To further clarify the 2DHG property at the interfaces, R_c is used to calculate the concentration (N_h) of 2DHG, due to the induced Ni nonalloyed ohmic contacts to p-AlGaN by a 2DHG channel. The relationship between R_c and N_h is expressed as

$$\begin{aligned} 16R_c &= \rho(L/S) \\ &= [t/(q\mu_h N_h)][L/(tW)] = L/(q\mu_h N_h W), \end{aligned} \tag{2}$$

where q is the electron charge, t is the thickness of 2DHG, W is the width of the recessed channels ($W = 20\,\mu m$), S is the cross-sectional area of the current from Ni into the 2DHG channel ($S = tW$), L is the transfer length ($0 < L < 20\,\mu m$, assuming $L = L_T = 347\,nm$), and μ_h is the mobility of 2DHG [assuming $\mu_h = 3.2\,cm^2/(V\,s)$]. Because of 4 recessed channels per p-pad electrode and 4 cross-sectional areas per recessed channel, we assume that 16 contact resistances per p-pad electrode are in parallel and the contact resistance is $16R_c$ ($16R_c = 16 \times 316\,\Omega$) per cross-sectional area. On the basis of our assumed model, N_h is calculated to be $6.7 \times 10^{12}\,cm^{-2}$, which implies that etching did not lead to a marked decrease in the concentration of 2DHG, due to activation annealing after etching. Cao *et al.*[20] suggested that annealing produced significant recovery of the electrical properties of GaN samples, after dry etching.

In summary, we have developed ohmic recessed technology using 2DHG caused by the polarization in the p-GaN capping layer grown on top of p-AlGaN as a way of forming nonalloyed ohmic contacts. The p-GaN capping layer grown on top of p-AlGaN led to the formation of spontaneous polarization fields and the lower band bending of p-AlGaN resulting in the formation of 2DHG. As a result, the concentration of free holes at the p-GaN/p-AlGaN interface is markedly increased and the lower band bending of p-GaN at the p-GaN/p-AlGaN interface is formed, thereby allowing for the enhancement of the hole injection in the p-AlGaN layer through the recessed channels and 2DHG channel. The application of ohmic recessed technology in the nonalloyed ohmic formation for p-AlGaN could be useful for improving the performance of flip-chip bonded UV LEDs.[7]

Acknowledgment

The author acknowledges support in the form of grants from the National Science Council of Taiwan, Republic of China (Contract No. NSC 94-2112-M-018-007).

1) M. A. Khan, M. Shatalov, H. P. Maruska, H. M. Wang and E. Kuokstis: Jpn. J. Appl. Phys. **44** (2005) 7191.
2) M. Osiński: *Gallium-Nitride-Based Technologies* (SPIE, Bellingham, WA, 2002).
3) J. Zhang, X. Hu, A. Lunev, J. Deng, Y. Bilenko, T. M. Katona, M. S. Shur, R. Gaska and M. A. Khan: Jpn. J. Appl. Phys. **44** (2005) 7250.
4) S. J. Pearton, J. C. Zolper, R. J. Shul and F. Ren: J. Appl. Phys. **86** (1999) 1.
5) H. Morkoç: *Nitride Semiconductors and Devices* (Springer, Berlin, 1999).
6) S. Nakamura and S. F. Chichibu: *Introduction to Nitride Semiconductor Blue Lasers and Light Emitting Diodes* (Taylor & Francis, London, 2000).
7) M. Khizar, Z. Y. Fan, K. H. Kim, J. Y. Lin and H. X. Jiang: Appl. Phys. Lett. **86** (2005) 173504.
8) B. A. Hull, S. E. Mohney, U. Chowdhury and R. D. Dupuis: J. Appl. Phys. **96** (2004) 7325.
9) B. H. Jun, H. Hirayama and Y. Aoyagi: Jpn. J. Appl. Phys. **41** (2002) 581.
10) B. A. Hull, S. E. Mohney, U. Chowdhury, R. D. Dupuis, D. Gotthold, R. Birkhahn and M. Pophristic: Mater. Res. Soc. Symp. Proc. **743** (2003) 12.2.1.
11) T. V. Blank, Y. A. Goldberg, E. V. Kalinina, O. V. Konstantinov, A. E. Nikolaev, A. V. Fomin and A. E. Cherenkov: Semiconductors **35** (2001) 529.
12) Th. Gessmann, J. W. Graff, Y. L. Li, E. L. Waldron and E. F. Schubert: J. Appl. Phys. **92** (2002) 3740.
13) Th. Gessmann, Y. L. Li, E. L. Waldron, J. W. Graff, E. F. Schubert and J. K. Sheu: J. Electron. Mater. **31** (2002) 416.
14) K. Kumakura, T. Makimoto and N. Kobayashi: Jpn. J. Appl. Phys. **42** (2003) 2254.
15) K. H. Kim, Z. Y. Fan, M. L. Nakarmi, J. Y. Lin and H. X. Jiang: Appl. Phys. Lett. **85** (2004) 4777.
16) Y. J. Lin: J. Vac. Sci. Technol. B **23** (2005) 48.
17) D. K. Schroder: *Semiconductor Material and Device Characterization* (John Wiley & Sons, New York, 1998) 2nd ed., p. 157.
18) Y. J. Lin: Appl. Phys. Lett. **86** (2005) 122109.
19) Y. J. Lin and Y. L. Chu: J. Appl. Phys. **97** (2005) 104904.
20) X. A. Cao, A. P. Zhang, G. T. Dang, F. Ren, S. J. Pearton, R. J. Shul and L. Zhang: J. Vac. Sci. Technol. A **18** (2000) 1144.

Enhancement of Schottky barrier height on *p*-type GaN by $(NH_4)_2S_x$ treatment

Yow-Jon Lin[a] and Chang-Feng You
Institute of Photonics, National Changhua University of Education, Changhua 500, Taiwan, Republic of China

Chi-Sen Lee
Graduate Institute of Electronics Engineering, National Taiwan University, Taipei 106, Taiwan, Republic of China

(Received 1 September 2005; accepted 19 January 2006; published online 6 March 2006)

Barrier height values of Ni contacts to $(NH_4)_2S_x$-treated *p*-type GaN (*p*-GaN) were obtained from current-voltage and x-ray photoelectron spectroscopy (XPS) measurements in this study. The induced deep level defect band through high Mg doping led to a reduction of the depletion layer width in the *p*-GaN near the interface and an increase in the probability of thermionic field emission (TFE). Furthermore, the calculated barrier height value of Ni contacts to $(NH_4)_2S_x$-treated *p*-GaN using the TFE model is close to the Schottky limit, which is in good agreement with the observed result by XPS measurements and suggests that $(NH_4)_2S_x$ surface treatment leads to the removal of native oxides and the reduction of the surface state related to oxygen-induced and nitrogen-vacancy defects. © *2006 American Institute of Physics*. [DOI: 10.1063/1.2175446]

I. INTRODUCTION

GaN is an attractive wide band-gap [3.4 eV direct gap at room temperature (RT)] semiconductor material for ultraviolet/visible (UV/VIB) optoelectronic devices. Other devices that have been demonstrated so far include UV photoconductive detectors, UV Schottky barrier photodetectors, metal-semiconductor field effect transistors, solar-blind Schottky photodiodes, and high electron mobility transistors.[1–6] High-quality Ohmic and Schottky contacts are required for the improvement of these devices. Because of the high work function for *p*-GaN, the high barrier height is expected after the deposited metals on *p*-GaN.[7] We have previously investigated the barrier of Ni on *p*-GaN and found that there was a larger tunneling component in the current transported across the junction under forward bias.[8] We found that the induced deep level defect band through high Mg doping led to a reduction of the depletion layer width in the *p*-GaN near the interface and an increase in the probability of thermionic field emission (TFE).[8] It resulted in an increase in current flow under forward bias condition, which was not analyzed using the thermionic emission (TE) model.[8] However, the calculated barrier height value of Ni contacts to *p*-GaN using the TFE model is lower than the Schottky limit. To improve the performance of Ni/*p*-GaN Schottky diodes in this study, $(NH_4)_2S_x$ treatment was used in the fabrication process. On the basis of the reported results,[9–11] we deduce that $(NH_4)_2S_x$ treatment may lead to the removal of native oxides and the reduction of surface states, resulting in the enhancement of Schottky barrier height ($q\phi_B$) for Ni/*p*-GaN Schottky diodes.

[a]Author to whom correspondence should be addressed; FAX: 886-4-7211153; electronic mail: rzr2390@yahoo.com.tw

II. EXPERIMENTAL PROCEDURE

The epitaxial layers used in the experiments were grown on *c*-plane sapphire substrates using a metal-organic chemical vapor deposition system. Trimethylgallium, ammonia, and biscyclopentadienylmagnesium were used as the Ga, N, and Mg sources, respectively. An undoped GaN buffer layer with a thickness of 650 nm was grown on the sapphire substrate at 520 °C, followed by the growth of a Mg-doped *p*-GaN layer (762 nm) at 1100 °C. Mg concentration [Mg] was $\sim 6 \times 10^{19}$ cm^{-3} for all samples. The [Mg] in *p*-GaN was measured by secondary ion mass spectroscopy. The [Mg] depth profile of *p*-GaN samples is shown in Fig. 1. The grown samples were annealed for the purpose of generating holes at 750 °C for 30 min in N_2 ambient. According to the Van der Pauw–Hall measurements, we found that the hole concentration was calculated to be 3.6×10^{17} cm^{-3}. The

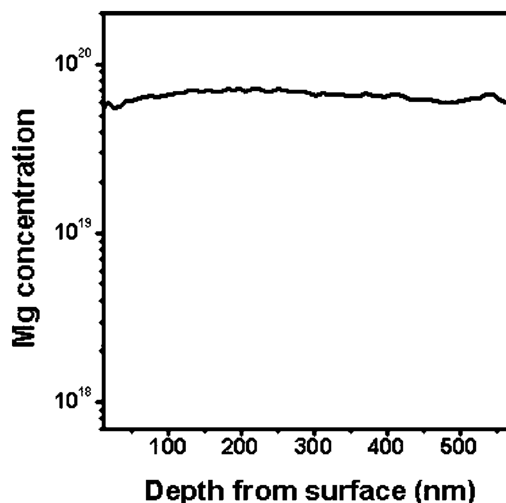

FIG. 1. [Mg] depth profiles of *p*-GaN samples.

 © 2006 American Institute of Physics

Downloaded 06 Mar 2006 to 163.23.208.249. Redistribution subject to AIP license or copyright, see http://jap.aip.org/jap/copyright.jsp

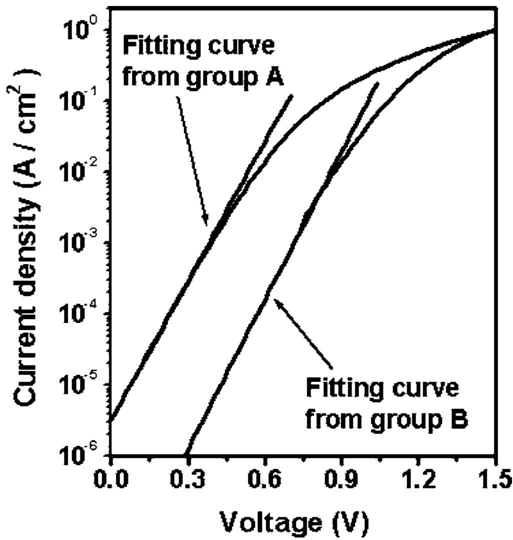

FIG. 2. *J-V* curve of Ni/*p*-GaN Schottky diodes under forward bias condition at 300 K and the fitting curve to the *J-V* characteristic in the TFE regime.

samples were cleaned in chemical clean solutions of trichloroethylene, acetone, and methanol. Planar-type Schottky contacts were formed by electron-beam evaporation. Using the lift-off technique, Ni/Au (5 nm/5 nm) ohmic contacts were deposited and annealed at 500 °C in air ambient for 10 min. The fabricated process of Ohmic contacts with the low specific contact resistance has been reported.[12] Next, Ni (5 nm) Schottky contacts with circular patterns (200 μm in diam eter) were directly deposited, which were referred to as group A. In addition, prior to the deposited Ni (5 nm) on Schottky contacts with circular patterns, the samples were dipped into the 60 °C-$(NH_4)_2S_x$ solution for 30 min,[11] which were referred to as group B. The current-voltage characteristics of Schottky diodes from groups A and B were measured using a Keithley Model-4200-SCS/F semiconductor characterization system.

III. EXPERIMENTAL RESULTS AND DISCUSSION

Figure 2 shows the typical semilog current density-voltage (*J-V*) characteristics of Ni/*p*-GaN Schottky diodes. The fitting curve using the TFE model is also shown in Fig. 2. The *J-V* characteristic in the presence of tunneling can be described by the relation[13,14]

$$J = J_O \exp(qV/E_O), \tag{1}$$

$$E_O = E_{OO} \coth(E_{OO}/kT), \tag{2}$$

$$J_O = \frac{A^* T[\pi E_{OO} q(\phi_B - V - \xi)]^{0.5}}{k \cosh(E_{OO}/kT)} \times \exp\left[-\frac{q\xi}{kT} - \frac{q}{E_O}(\phi_B - \xi)\right], \tag{3}$$

$$E_{OO} = (qh/4\pi)(N/m^* \varepsilon)^{0.5}, \tag{4}$$

where J is the observed current density of Schottky diodes of group A or B under forward bias condition, m^* ($m^*=0.6\, m_o$, m_o is the mass of hole at rest)[15] is the hole effective mass, ε ($\varepsilon=9.5\varepsilon_o$, ε_o is the permittivity in vacuum)[16] is the dielectric constant of GaN, A^* ($A^*=103.8$ A/cm^2 K^2) is the effective Richardson constant[17] of the *p*-GaN, h is Planck's constant, V is voltage, q is the electron charge, N is the doping concentration, and ξ is equal to $(E_F\text{-}E_V)/q$. E_V is the valence-band maximum and E_F is the position of the Fermi level. Nakayama *et al.*[18] suggested that hole concentration of 2×10^{17} cm^{-3} in *p*-GaN samples led to ξ=0.13 V. As a result, we deduce that hole concentration of 3.6×10^{17} cm^{-3} in *p*-GaN samples, used in this study, may result in ξ <0.13 V. Consequentially, ξ was assumed to be equal to 0.1 V in this study. According to the fitting J vs V curve of samples from group A using Eqs. (1)–(3), the value of E_O, E_{OO}, and $q\phi_B$ can be calculated to be 66 meV, 65 meV, and 1.8 eV, respectively. Similarly, according to the fitting J vs V curve of samples from group B using Eqs. (1)–(3), the value of E_O, E_{OO}, and $q\phi_B$ can be calculated to be 61 meV, 60 meV, and 2.1 eV, respectively. Then, the calculated value ($6\sim7\times10^{19}$ cm^{-3}) of N for samples from group A or B using Eq. (4) is similar to [Mg], which indicated that the tunneling current under forward bias conditions took place because of the high Mg doping [or the deep level defect (DLD) band induced by high Mg doping].[19,20] Kwak *et al.*[19]have suggested that the current transport at the metal/high Mg-doped *p*-GaN interface was dominated by a DLD band which was induced by high Mg doping. Kwak *et al.*[20] have also suggested that the DLD band had a large density defect, over 10^{19} cm^{-3} size, existing in the *p*-GaN films and that the density of the DLDs increased as [Mg] increased. In addition, Shiojima *et al.*[21] have found carrier capture and emission from acceptorlike DLDs for Ni/*p*-GaN Schottky diodes. Further, it is worth noting that the calculated value of E_{OO}/kT is slightly larger than 1, which implies the current transport processes a tunnel component.[14] On the other hand, the observed current is too small to obtain the fitting parameters for the *J-V* characteristic in the field emission (FE) regime for Ni/*p*-GaN samples from groups A and B. This suggests that the FE model cannot be used to study the $q\phi_B$ of Ni/*p*-GaN in this case. In addition, the E_{OO} of samples from group A or B is not much greater than kT (kT $=26$ meV, at 300 K), so the FE will not take place.[13] The effective resistance of the Schottky barrier in the FE regime is quite low, so the FE model is often used for Ohmic contact.[13]

On the other hand, the calculated $q\phi_B$ of samples from groups A and B by Eq. (3) is 1.80 and 2.1 eV, respectively. However, we found that the barrier height (2.1 eV) of Ni contacts to $(NH_4)_2S_x$-treated *p*-GaN is close to the Schottky limit of 2.3 eV. For *p*-type semiconductors, the ideal $q\phi_B$ is given by[22]

$$q\phi_B = \chi + E_g - q\phi_m, \tag{5}$$

where $q\phi_m$=5.2 eV is the work function of Ni,[23] χ (χ $=4.1$ eV) is the electron affinity[24] of GaN, and E_g (E_g $=3.4$ eV) represents the band gap of GaN. According to Eq. (5), the Schottky limit could be calculated to be 2.3 eV. The fact that the $q\phi_B$ improved suggests that $(NH_4)_2S_x$ treatment is effective in removing the native oxides, reducing the sur-

Downloaded 06 Mar 2006 to 163.23.208.249. Redistribution subject to AIP license or copyright, see http://jap.aip.org/jap/copyright.jsp

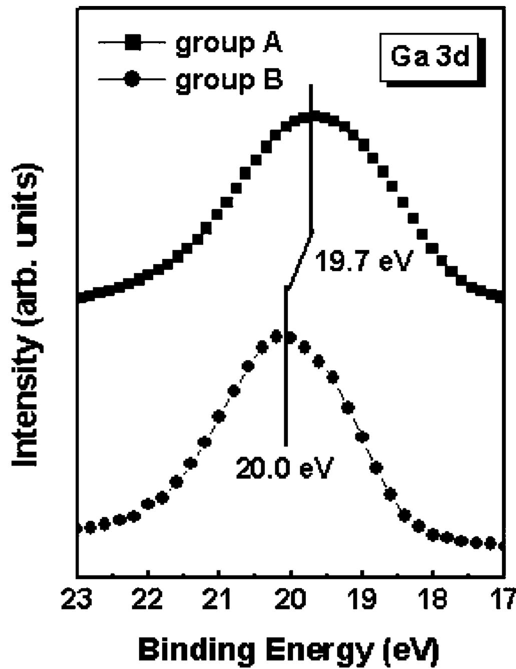

FIG. 3. Ga 3d core level at the Ni/p-GaN interface. The binding energy is referenced to the Fermi level.

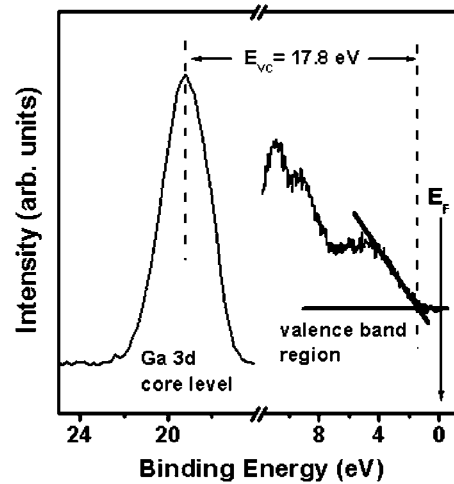

FIG. 4. The left-hand spectrum shows the Ga 3d core-level peak on p-GaN without a Ni overlayer. The right-hand figure presents the spectrum of the valence-band region. A linear fit is used to determine the energy of the valence-band edge.

face state related to oxygen-induced, contamination-induced, and nitrogen-vacancy defects, and passivating the surface of p-GaN.[9–11]

In order to further confirm whether the calculated $q\phi_B$ of Ni/$(NH_4)_2S_x$-treated p-GaN Schottky diodes is reasonable or not, x-ray photoelectron spectroscopy (XPS) is used to study the position of Ga 3d core-level peak for samples from groups A and B. XPS measurements were performed using a monochromatic Al K_α x-ray source. We took a Au $4f_{7/2}$ peak and a Cu $2p_{3/2}$ peak for energy reference purposes. Figure 3 shows the Ga 3d core-level XPS spectra at the Ni/p-GaN interfaces. We find that the Ga 3d core-level peaks of samples from groups A and B ($E_{\mathrm{Ga}\ 3d}$) are located at 19.7 and 20.0 eV, respectively. Compared to samples from group A, the $(NH_4)_2S_x$ treatment produced the Ga 3d core-level peaks which were 0.3 eV closer toward the conduction-band edge, which leads to bigger $q\phi_B$. This is in good agreement with our observed results from the J-V measurements and suggests that the near-ideal p-GaN surface can be obtained after the $(NH_4)_2S_x$ treatment. When Ni and $(NH_4)_2S_x$-treated p-GaN are in intimate contact, the $q\phi_B$ will be more sensitive to the metal work function. This explained why the $q\phi_B$ of samples from group B is close to the Schottky limit. In addition, Shalish *et al.*[25] indicated that the removal of GaO_x led to the removal of induced surface states by GaO_x. Reshchikov *et al.*[26] suggested that the GaN surface oxidized in air, resulting in a band bending caused by the charge localized at the surface states associated with oxygen-induced states. In a previous study,[9] we found that $(NH_4)_2S_x$ treatment resulted in the reduction of nitrogen-vacancy-related surface states. As a result, we suggest that $(NH_4)_2S_x$ treatment may lead to the removal of GaO_x and the reduction of the surface states associated with GaO_x, oxygen-induced states and nitrogen-vacancy-related surface states, which result in the reduction of the leakage current related to the direct tunneling or indirect tunneling via states, and E_O (or E_{OO}).

Figure 4 shows an example of the Ga 3d core level and the valence-band spectrum collected on a p-GaN sample without a Ni overlayer.[8] For the calculation of $q\phi_B$ of samples from group A or B, the equation is expressed as[8]

$$q\phi_B = E_{\mathrm{Ga}\ 3d} - E_{\mathrm{VC}}. \tag{6}$$

The E_{VC} is calculated to be 17.8 eV, as shown in Fig. 4, which is in good agreement with the value of 17.8 eV reported by Bermudez[27] and Wu and Kahn.[28] In Fig. 3, we can see that the $E_{\mathrm{Ga}\ 3d}$ of samples from groups A and B are equal to 19.7 and 20.0 eV, respectively. Therefore, the $q\phi_p$ of samples from groups A and B were calculated to be 1.9 and 2.2 eV, according to Eq. (6), which is in good agreement with the obtained result from J-V measurements.

IV. CONCLUSIONS

In summary, the barrier height values of Ni contacts to p-GaN with and without $(NH_4)_2S_x$ treatment were obtained from J-V and XPS measurements in this study. Excellent agreement between simulated and measured data was obtained when the tunneling component in the transport current was taken into account. For the Ni/$(NH_4)_2S_x$-treated p-GaN Schottky diodes, the calculated barrier height value using the TFE model is close to the Schottky limit, which is in good agreement with the observed result by XPS measurements and suggests that $(NH_4)_2S_x$ surface treatment leads to the removal of surface oxides and the reduction of the surface state related to oxygen-induced, contamination-induced, and nitrogen-vacancy defects.

ACKNOWLEDGMENT

This project is supported by the National Science Council of Taiwan, Republic of China under contract No. NSC94-2112-M-018-007.

Downloaded 06 Mar 2006 to 163.23.208.249. Redistribution subject to AIP license or copyright, see http://jap.aip.org/jap/copyright.jsp

[1]M. A. Khan, J. N. Kuznia, D. T. Olson, J. M. Van Hove, and M. Blasingame, Appl. Phys. Lett. **60**, 2917 (1992).
[2]O. Katz, V. Garber, B. Meyler, G. Bahir, and J. Salzman, Appl. Phys. Lett. **79**, 1417 (2001).
[3]M. A. Khan, J. N. Kuznia, D. T. Olson, M. Blasingame, and A. R. Bhattarai, Appl. Phys. Lett. **63**, 2455 (1993).
[4]M. A. Khan, J. N. Kuznia, A. R. Bhattarai, and D. T. Olson, Appl. Phys. Lett. **62**, 1786 (1993).
[5]N. Biyikli, O. Aytur, I. Kimukin, T. Tut, and E. Ozbay, Appl. Phys. Lett. **81**, 3272 (2002).
[6]M. A. Khan, A. R. Bhattarai, J. N. Kuznia, and D. T. Olson, Appl. Phys. Lett. **63**, 1214 (1993).
[7]M. W. Wang, J. O. McCaldin, J. F. Swenberg, T. C. McGill, and R. J. Hauenstein, Appl. Phys. Lett. **66**, 1974 (1995).
[8]Y. J. Lin, Appl. Phys. Lett. **86**, 122109 (2005).
[9]Y. J. Lin, Z. L. Wang, and H. C. Chang, Appl. Phys. Lett. **81**, 5183 (2002).
[10]Y. J. Lin, Y. L. Chu, Y. S. Huang, and H. C. Chang, Appl. Phys. Lett. **86**, 202107 (2005).
[11]Y. J. Lin, C. D. Tsai, Y. T. Lyu, and C. T. Lee, Appl. Phys. Lett. **77**, 687 (2000).
[12]J. K. Ho, C. S. Jong, C. N. Huang, C. Y. Chen, C. C. Chiu, and K. K. Shih, Appl. Phys. Lett. **74**, 1275 (1999).
[13]Michael Shur, *Physics of Semiconductor Devices* (Prentice-Hall, Englewood Cliffs, NJ, 1990).
[14]H. Morkoç, *Nitride Semiconductors and Devices* (Springer, Berlin, 1999).
[15]C. Merz, M. Kunzer, U. Kaufmann, I. Akasaki, and H. Amano, Semicond. Sci. Technol. **11**, 712 (1996).
[16]M. Razeghi and A. Rogalski, J. Appl. Phys. **79**, 7433 (1996).
[17]J. I. Pankove, S. Bloom, and G. Harbeke, RCA Rev. **36**, 163 (1975).
[18]H. Nakayama, P. Hacke, M. R. H. Khan, T. Detch-Prohm, K. Hirmatsu, and N. Sawaki, Jpn. J. Appl. Phys., Part 2 **35**, L282 (1996).
[19]J. S. Kwak, O. H. Nam, and Y. Park, Appl. Phys. Lett. **80**, 3554 (2002).
[20]J. S. Kwak, O. H. Nam, and Y. Park, J. Appl. Phys. **95**, 5917 (2004).
[21]K. Shiojima, T. Sugahara, and S. Sakai, Appl. Phys. Lett. **77**, 4353 (2000).
[22]B. L. Sharma, *Metal-Semiconductor Schottky Barrier Junctions and Their Applications* (Plenum, New York, 1984).
[23]H. B. Michaelson, IBM J. Res. Dev. **22**, 72 (1978).
[24]S. Arulkumaran, T. Egawa, H. Ishikawa, T. Jimbo, and M. Umeno, Appl. Phys. Lett. **73**, 809 (1998).
[25]I. Shalish, Y. Shapira, L. Burstein, and J. Salzman, J. Appl. Phys. **89**, 390 (2001).
[26]M. A. Reshchikov, P. Visconti, and H. Morkoç, Appl. Phys. Lett. **78**, 177 (2001).
[27]V. M. Bermudez, J. Appl. Phys. **80**, 1190 (1996).
[28]C. I. Wu and A. Kahn, J. Appl. Phys. **86**, 3209 (1999).

Downloaded 06 Mar 2006 to 163.23.208.249. Redistribution subject to AIP license or copyright, see http://jap.aip.org/jap/copyright.jsp

Japanese Journal of Applied Physics
Vol. 45, No. 4A, 2006, pp. 2505–2508

©2006 The Japan Society of Applied Physics

Electronic Transport and Schottky Barrier Heights of Ni/Au Contacts on n-Type GaN Surface with and without a Thin Native Oxide Layer

Yow-Jon LIN*, Wen-Xiang LIN, Ching-Ting LEE[1] and Hsing-Cheng CHANG[2]

Institute of Photonics, National Changhua University of Education, Changhua 500, Taiwan, Republic of China
[1]*Institute of Microelectronics, Department of Electrical Engineering, National Cheng-Kung University, Tainan 701, Taiwan, Republic of China*
[2]*Department of Automatic Control Engineering, Feng Chia University, Taichung 407, Taiwan, Republic of China*

(Received November 8, 2005; accepted December 23, 2005; published online April 7, 2006)

Effects of a thin native oxide layer on Au/Ni/n-type GaN Schottky diodes were investigated in this study. The tunneling current was induced in the presence of native oxides on the GaN surface, making the thermionic emission (TE) theory inapplicable in this case. We find that the value of the barrier height (BH) calculated using the thermionic field emission (TFE) model is similar to that obtained by capacitance–voltage characteristics. This suggested that the discrepancy between BH according to the TFE and TE model for Au/Ni/n-type GaN Schottky diodes could be attributed to the presence of a native oxide layer at the Ni/n-type GaN interface and oxygen-induced and nitrogen-vacancy-related states on the GaN surfaces. Further, the characteristics of Schottky diodes improved when the n-type GaN was treated with $(NH_4)_2S_x$ solution, an effective agent for removing native oxides and reducing surface states. [DOI: 10.1143/JJAP.45.2505]

KEYWORDS: GaN, Schottky barrier height, thermionic field emission, thermionic emission, surface treatment

1. Introduction

GaN has a 3.4 eV direct gap at room temperature and attracted much interest because of its application in optical devices in the short-wavelength region. Other devices that have been demonstrated so far include ultraviolet photoconductive detectors, ultraviolet Schottky barrier photodetectors, metal–semiconductor field effect transistors, and Schottky diode gas sensors.[1–6] High-quality ohmic and Schottky contacts are required for the improvement of these devices. Excellent ohmic contacts on n-type GaN (n-GaN) utilizing Ti/Al have been reported.[7] Regarding Schottky contacts, recent investigations have described the barrier heights of Au,[8,9] Pt,[8,10] and Pd[10,11] on n-GaN. However, most Schottky diodes have thin layers of native oxide at the metal–semiconductor junction, unless all the processing is done in a vacuum. To improve advancement of these devices, the electrical properties of the interface (i.e., thin native oxide) have to be fully investigated. Better knowledge of the Schottky barrier and interfacial effects of thin native oxides for the n-GaN Schottky diodes is needed. Cao *et al.*[12] have suggested that this thin oxide influences the contact characteristics on GaN and appears to be responsible for some of the wide spread in contact properties. However, the relationship between the tunneling current and thin native oxide was not taken into account in their simple model.[12] In this study, a thermionic field emission (TFE) model involving the presence of thin native oxides is proposed to account for the larger currents observed under forward-bias conditions. We find that these analytic results strongly indicate that a TFE model can quantitatively explain the larger observed forward currents. Our experimental results suggest that the oxide layer and surface states (i.e., oxygen-induced and nitrogen-vacancy-related states) lead to the formation of the tunneling component of the current through the barrier. Further, the presence of the tunneling component in the transport current results in a decreased observed barrier height and increased observed ideality factor (n) according to the thermionic emission (TE) model, which is in agreement with the reported results by Sawada *et al.*[13] Sawada *et al.*[13] indicated that these additional currents seem to modify the TE current and apparently lower the Schottky barrier height from current–voltage (I–V) measurements.

2. Experimental

The epitaxial layers used in this study were grown on c-plane sapphire (0001) by the metalorganic chemical vapor deposition technique. An undoped GaN layer with a thickness of 650 nm was grown on the sapphire substrate at 520 °C, followed by a 1.2-μm-thick n-GaN layer doped with Si, at 1050 °C. According to the Hall measurement at room temperature, the n-type carrier concentration and mobility were 5×10^{17} cm^{-3} and 350 cm^2 V^{-1} s^{-1}, respectively. Next, with a Ni/Au (50/600 nm) metal mask, circular mesa regions with a diameter of 400 μm were patterned by a reactive ion etching system using BCl_3 etchant. The etched depth was approximately 500 nm. The sample was then divided into Groups A and B. Both groups were cleaned with chemical solutions of trichlorethylene, acetone and methanol. The cleaned samples were then dipped into a yellow $(NH_4)_2S_x$ solution (with 6% of S) at 60 °C for 20 min. After the Ni/Au metal mask was removed, Ti/Al (50/150 nm) metals were deposited using an electron beam evaporator. With the lift-off technique, the ohmic metals of Ti/Al in contact with the etched n-GaN region were preformed and then alloyed using a thermal annealing furnace in N_2 ambient, at 300 °C for 4 min. The specific contact resistance of 3×10^{-6} Ω cm^2 was obtained. To investigate the characteristics of Ni/Au Schottky contacts on n-GaN with and without thin native oxide prior to the deposition of Ni/Au (20/200 nm) Schottky metals, samples from Group A were dipped into the same $(NH_4)_2S_x$ solution mentioned above at 60 °C for 20 min. Then, circular Ni/Au pads with a diameter of 400 μm, in contact with the mesa regions of Groups A and B, were fabricated using the lift-off technique. The I–V characteristics of Schottky diodes were measured using a Keithley Model-4200-SCS/F semiconductor characterization system.

3. Results and Discussion

Figure 1 shows the forward I–V characteristics of Schottky diodes. The fitting curve of the I–V characteristics

*Corresponding author. E-mail address: rzr2390@yahoo.com.tw

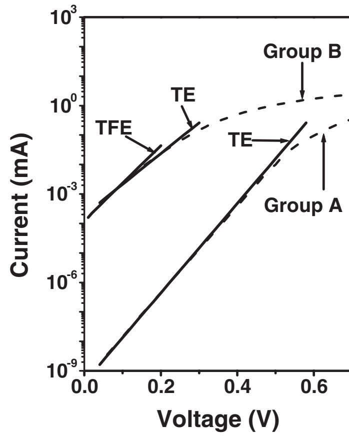

Fig. 1. Forward *I–V* characteristics of Schottky diodes.

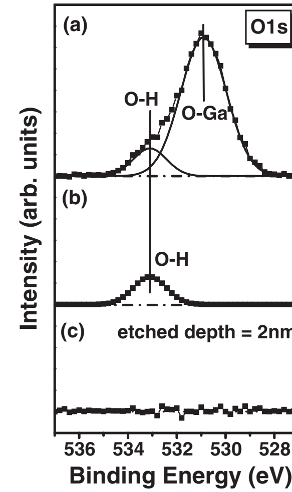

Fig. 2. O 1s core-level XPS spectra of (a) as-cleaned n-GaN, (b) $(NH_4)_2S_x$-treated n-GaN, and (c) etched as-cleaned n-GaN.

in the TE regime is also shown in Fig. 1. The barrier heights and ideality factors were obtained from the forward *I–V* characteristics, according to the equation of $I = SA^{**}T^2 \exp(-q\phi_b/kT)\exp(qV/nkT)[1-\exp(-qV/kT)]$.[12] S is the contact area, T is the measurement temperature, k is the Boltzmann constant, q is the electron charge, A^{**} is the effective Richardson constant (26.4 $A\,cm^{-2}\,K^{-2}$ for n-type GaN)[12] and $q\phi_b$ is the measured barrier height. By fitting a linear curve to the forward characteristics in Fig. 1, $q\phi_b$ and n can be calculated. $q\phi_b$ for Groups A and B is 0.97 and 0.62 eV, respectively; while n for Groups A and B is 1.1 and 1.6, respectively. When we took into account the image-force lowering ($\Delta\phi$) effect,[9] the effective barrier height ($q\phi, q\phi = q\phi_b + q\Delta\phi$) for Groups A and B was corrected to be 1.05 and 0.70 eV, respectively. If the work function of Ni is 5.20 eV[14] and the electron affinity of GaN is 4.10 eV,[15] the Schottky limit for the Au/Ni/n-GaN calculated will be 1.10 eV. For Au/Ni/$(NH_4)_2S_x$-treated n-GaN, we found that the effective barrier height is close to the Schottky limit of 1.10 eV. An explanation for this will be given later.

To study the interfacial mechanism of the barrier formation for Ni/Au bilayer contacts to the as-cleaned (i.e., Group B) and $(NH_4)_2S_x$-treated (i.e., Group A) n-GaN surface, the GaN surfaces with and without $(NH_4)_2S_x$ treatment were analyzed using X-ray photoelectron spectroscopy (XPS) employing a monochromatic Mg $K\alpha$ X-ray source. We took a Au $4f_{7/2}$ peak and Cu $2p_{3/2}$ peak for energy reference purposes. The O 1s core-level peaks were de-convolved into their various components using an interactive least-squares computer program; the curves were taken as 80% Gaussian and 20% Lorentzian mixed functions. XPS analysis can be combined with argon ion sputter etching to obtain the depth profile for the interfacial layer. Figure 2 shows the O 1s XPS spectra of as-cleaned n-GaN, $(NH_4)_2S_x$-treated n-GaN and etched as-cleaned n-GaN. It can be seen that a few O–H bonds (533.1 eV)[7] existed on the $(NH_4)_2S_x$-treated n-GaN surface. It can also be seen that O–Ga (530.8 eV)[7] and a few O–H bonds (533.1 eV) existed on the as-cleaned GaN surface. When the etched depth of the as-cleaned n-GaN sample was about 2 nm, no O 1s signal existed on the etched n-GaN surface. From this we can deduce that the thickness of the native oxide layer is less than 2 nm. It is worth noting that the transport current of Ni/Au contacts to n-GaN with native oxide is larger than that of Ni/Au contacts to $(NH_4)_2S_x$-treated n-GaN. In general, the presence of oxides will lead to an increase in the contact resistance and the reduction of the transport current. This suggested that the native oxide (i.e., GaO_x) present at the Ni/n-GaN interface resulted in the excess current component related to the direct tunneling or indirect tunneling via states present in the thin oxide layer and at the oxides/n-GaN interface, which led to the degradation of the Schottky diode. We deduced that a TE model was used to obtain the lower barrier height and larger ideality factor in this case. In addition, Shalish *et al.*[16] indicated that the removal of GaO_x led to the reduction of the emitted yellow luminescence from surface states associated with GaO_x. Reshchikov *et al.*[17] suggested that the GaN surface oxidized in air, resulting in a band-bending caused by the charge localized at the surface states associated with oxygen-induced states. In a previous study,[18] we found that $(NH_4)_2S_x$ treatment resulted in the reduction of nitrogen-vacancy-related surface states. As a result, we deduce that $(NH_4)_2S_x$ treatment may lead to the removal of GaO_x and the reduction of the surface states associated with GaO_x, oxygen-induced states and nitrogen-vacancy-related surface states, which results in the reduction of the leakage current related to the direct tunneling or indirect tunneling via states. According to these reports,[19–21] due to the existence of interface states in a thin oxide between the metal and the semiconductor, the ideality factor would be more than 1. These reports[22,23] provide a theoretical analysis of the tunneling component of the current through a Schottky barrier. In TFE, the tunneling component of the current can be written as[22,23]

$$I_B = I_O \exp(qV/E_O) \quad (1)$$

$$E_O = E_{OO} \coth(E_{OO}/kT) \quad (2)$$

$$I_O = \frac{SA^*T[\pi E_{OO} q(\phi_T - V - \xi)]^{0.5}}{k\cosh(E_{OO}/kT)} \times \exp\left[-\frac{q\xi}{kT} - \frac{q}{E_O}(\phi_T - \xi)\right] \quad (3)$$

where I_B is the measured current of Schottky diode from Group B and $q\phi_T$ is the barrier height obtained from the TFE model. ξ is equal to $(E_C - E_F)/q = (kT/q)\ln(N_c/N_d)$. E_C is

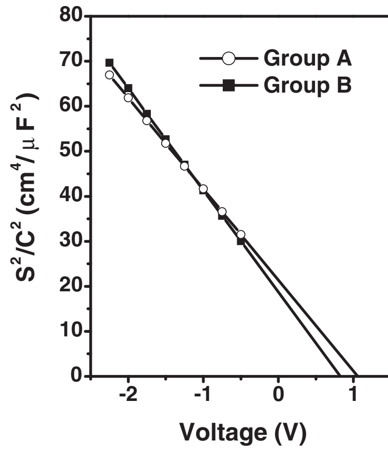

Fig. 3. S^2/C^2–V plot of Schottky diodes.

the energy of conduction band edge, E_F is the energy of Fermi level, and $N_c = 2.53 \times 10^{18}$ cm^{-3} is the effective density of states in the conduction band of n-GaN.[24] The fitting curve of the I–V characteristics in the TFE regime is shown in Fig. 1. By fitting I vs V curve and using eqs. (1)–(3), the values of E_O, E_{OO}, and $q\phi_T$ are calculated to be 0.034, 0.025, and 0.851 eV, respectively. It is worth noting that the calculated value of E_{OO}/kT is close to 1. This indicated that a mixture of TE and tunneling mechanism is indeed observed.[23] This observation led us to suggest that the presence of the thin native oxide resulted in the formation of the tunneling component in the transport current. Sawada *et al.*[13] indicated that these additional currents seem to modify the TE current and apparently lower the Schottky barrier height from I–V measurements. On the other hand, we find that that the Fermi level of n-GaN at the interface shifts toward the conduction band due to the existence of the native oxide. However, the increased leakage current for samples from Group B could not be directly explained by the movement of the surface Fermi level, because the ideality factor ($n = 1.6$) of samples from Group B was calculated to be more than 1 (based on the TE model). Consequently, we suggest that the existence of the native oxide and induced donor-type defects on the n-GaN surfaces led to an increase in the probability of tunneling, resulting in the increase of leakage currents. After $(NH_4)_2S_x$ treatment, we discovered that the native oxides were removed. This would cause the domination of TE in the transmission of electrons at this interface in the absence of native oxides.

On the other hand, the capacitance–voltage (C–V) characteristic of the Schottky diode was measured using an HP4280A 1 MHz C meter/C–V plotter.[18] The measured S^2/C^2 as a function of applied voltage V for the Schottky diode of Groups A and B is shown in Fig. 3.[18] The C–V relationship for a Schottky diode with a negligible oxide layer between the metal and the semiconductor is given by:[24]

$$S^2/C^2 = (2/\varepsilon_s q N_d)(V_i - V) \tag{4}$$

where $\varepsilon_s = 9.5\varepsilon_0$ for GaN, ε_0 is the permittivity in vacuum, N_d is the carrier concentration, and V_i is the x intercept at $1/C^2 = 0$. According to eq. (4), from the slope of Fig. 3, the carrier concentration of 7.4×10^{17} and 6.2×10^{17} cm^{-3} for Groups A and B were calculated, respectively. These values are similar to those obtained from the Hall measurement. The difference in carrier concentration between Groups A and B is attributed to the increase in carrier concentration due to the surface treatment of $(NH_4)_2S_x$.[18,25,26] The Schottky barrier height $q\phi_B$ is related to V_i by the relationship:

$$q\phi_B = qV_i + kT + q\xi \tag{5}$$

The Schottky barrier height $q\phi_B$ for Groups A and B is 1.099 and 0.856 eV, respectively. $q\phi_B$ (= 1.099 eV) of samples from Group A is similar to $q\phi$ (= 1.05 eV) of the same samples. On the other hand, $q\phi_B$ (= 0.856 eV) of samples from Group B is similar to $q\phi_T$ (= 0.851 eV) and is larger than the $q\phi$ (= 0.70 eV) of the same samples, because the presence of the induced tunneling component by a thin oxide layer existing at the Ni/n-GaN interface does not be considered for the barrier-height calculation according to the TE model, resulting in the formation of the larger n than 1 and the occurrence of the underestimated Schottky barrier height calculated from TE model. All observed Schottky characteristics of samples from Groups A and B were summarized in Table I.

4. Conclusions

In summary, the effects of a thin native oxide layer on the performances of the Au/Ni/n-GaN Schottky diodes have been investigated. The presence of native oxides (i.e., GaO_x) and surface states associated with oxygen-induced and nitrogen-vacancy-related states resulted in the formation of the tunneling component of the current through the barrier and the degradation of the Schottky characteristics. Excellent agreement between simulated and measured data was obtained when the tunneling component in the transport current was taken into account. In addition, Oyama *et al.*[27] have found that the tunneling plays an important role in the carrier transport across the n-GaN Schottky barrier even for doping densities as low as 10^{17} cm^{-3}, from the calculation about the reverse biased I–V characteristics based on the TFE model. However, samples which had undergone $(NH_4)_2S_x$ treatment showed a complete removal of thin native oxide, the reduction of surface states, and the domination of TE in the transmission of electrons at the interface.

Table I. Schottky barrier heights, ideality factors (n) and tunneling parameter (E_{OO}/kT) for Ni/Au Schottky contacts on n-GaN.

	I–V (TE) n	I–V (TE) $q\phi_b$ (eV)	I–V (TE) $q\phi_b + \Delta\phi = q\phi$ (eV)	I–V (TFE) $q\phi_T$ (eV)	I–V (TFE) E_{OO}/kT (300 K)	C–V $q\phi_B$ (eV)
Group A	1.1	0.97	1.05	—	—	1.099
Group B	1.6	0.62	0.7	0.851	∼1	0.856

Acknowledgment

The authors wish to acknowledge support by grants from National Science Council of Taiwan, Republic of China (Contract No. NSC 94-2112-M-018-007).

1) A. Motogaito, M. Yamaguchi, K. Hiramatsu, M. Kotoh, Y. Ohuchi, K. Tadatomo, Y. Hamamura and K. Fukui: Jpn. J. Appl. Phys. **40** (2001) L368.
2) Y. Kokubun, T. Seto and S. Nakagomi: Jpn. J. Appl. Phys. **40** (2001) L663.
3) M. A. Khan, D. T. Olson, J. N. Kuznia, A. R. Bhattarai and S. Krishnankutty: Inst. Phys. Conf. Ser. **137** (1993) 519.
4) O. Katz, V. Garber, B. Meyler, G. Bahir and J. Salzman: Appl. Phys. Lett. **79** (2001) 1417.
5) H. Morkoç, A. D. Carlo and R. Cingolani: Solid-State Electron. **46** (2002) 157.
6) B. P. Luther, S. D. Wolter and S. E. Mohney: Sens. Actuators B **56** (1999) 164.
7) Y. J. Lin, H. Y. Lee, F. T. Hwang and C. T. Lee: J. Electron. Mater. **30** (2001) 532.
8) Y. Koyama, T. Hamotsu and H. Hasegawa: Solid-State Electron. **43** (1999) 1483.
9) S. K. Noh and P. Bhattacharya: Appl. Phys. Lett. **78** (2001) 3642.
10) L. Wang, M. I. Nathan, T. H. Lim, M. A. Khan and Q. Chen: Appl. Phys. Lett. **68** (1996) 1267.
11) H. Ishikawa, K. Nakamura, T. Egawa, T. Jimbo and M. Umeno: Jpn. J. Appl. Phys. **37** (1998) L7.
12) X. A. Cao, S. J. Pearton, G. Dang, A. P. Zhang, F. Ren and J. M. Van Hove: Appl. Phys. Lett. **75** (1999) 4130.
13) M. Sawada, T. Sawada, Y. Yanagata, K. Imai, H. Kimura, M. Yoshino, K. Iizuka and H. Tomozawa: J. Cryst. Growth **189–190** (1998) 706.
14) H. B. Michaelson: IBM J. Res. Dev. **22** (1978) 72.
15) S. Arulkumaran, T. Egawa, H. Ishikawa, T. Jimbo and M. Umeno: Appl. Phys. Lett. **73** (1998) 809.
16) I. Shalish, Y. Shapira, L. Burstein and J. Salzman: J. Appl. Phys. **89** (2001) 390.
17) M. A. Reshchikov, P. Visconti and H. Morkoç: Appl. Phys. Lett. **78** (2001) 177.
18) C. T. Lee, Y. J. Lin and D. S. Liu: Appl. Phys. Lett. **79** (2001) 2573.
19) J. H. Werner, A. F. J. Levi, R. T. Tung, M. Anzlower and M. Pinto: Phys. Rev. Lett. **60** (1988) 53.
20) H. C. Card and E. H. Rhoderick: J. Phys. D **4** (1971) 1589.
21) J. H. Werner, K. Ploog and H. J. Queisser: Phys. Rev. Lett. **57** (1986) 1080.
22) M. Shur: *Physics of Semiconductor Devices* (Prentice-Hall, Englewood Cliffs, NJ, 1990).
23) H. Morkoç: *Nitride Semiconductors and Devices* (Springer, Berlin, 1999).
24) P. Hacke, T. Detchprohm, K. Hiramatsu and N. Sawaki: Appl. Phys. Lett. **63** (1993) 2676.
25) G. L. Martinez, M. R. Curiel, B. J. Skromme and R. J. Molnar: J. Electron. Mater. **29** (2000) 325.
26) P. Moriarty, B. Murphy, L. Roberts, A. A. Cafolla, G. Hughes, L. Koenders and P. Bailey: Phys. Rev. B **50** (1994) 14237.
27) S. Oyama, T. Hashizume and H. Hasegawa: Appl. Surf. Sci. **190** (2002) 322.